# *Drosophila* Bestrophin-1 Chloride Current Is Dually Regulated by Calcium and Cell Volume

Li-Ting Chien and H. Criss Hartzell

Department of Cell Biology and Center for Neurodegenerative Disease, Emory University School of Medicine, Atlanta, GA 30322

Mutations in the human bestrophin-1 (*hBest1*) gene are responsible for Best vitelliform macular dystrophy, however the mechanisms leading to retinal degeneration have not yet been determined because the function of the bestrophin protein is not fully understood. Bestrophins have been proposed to comprise a new family of $Cl^-$ channels that are activated by $Ca^{2+}$. While the regulation of bestrophin currents has focused on intracellular $Ca^{2+}$, little is known about other pathways/mechanisms that may also regulate bestrophin currents. Here we show that $Cl^-$ currents in *Drosophila* S2 cells, that we have previously shown are mediated by bestrophins, are dually regulated by $Ca^{2+}$ and cell volume. The bestrophin $Cl^-$ currents were activated in a dose-dependent manner by osmotic pressure differences between the internal and external solutions. The increase in the current was accompanied by cell swelling. The volume-regulated $Cl^-$ current was abolished by treating cells with each of four different RNAi constructs that reduced dBest1 expression. The volume-regulated current was rescued by transfecting with dBest1. Furthermore, cells not expressing dBest1 were severely depressed in their ability to regulate their cell volume. Volume regulation and $Ca^{2+}$ regulation can occur independently of one another: the volume-regulated current was activated in the complete absence of $Ca^{2+}$ and the $Ca^{2+}$-activated current was activated independently of alterations in cell volume. These two pathways of bestrophin channel activation can interact; intracellular $Ca^{2+}$ potentiates the magnitude of the current activated by changes in cell volume. We conclude that in addition to being regulated by intracellular $Ca^{2+}$, *Drosophila* bestrophins are also novel members of the volume-regulated anion channel (VRAC) family that are necessary for cell volume homeostasis.

The Journal of General Physiology

## INTRODUCTION

Mutations in human bestrophin-1 (*hBest1*) are genetically linked to a juvenile-onset macular degeneration called Best vitelliform macular dystrophy (Best disease) (Petrukhin et al., 1998; Marquardt et al., 1998). Mutations in the *hBest1* gene are also associated with a small fraction of cases of adult onset vitelliform macular dystrophy (Allikmets et al., 1999; Kramer et al., 2000) and autosomal dominant vitreoretinochoroidopathy (Yardley et al., 2004). The underlying mechanisms of these disorders are still unknown, mainly because the basic function of the bestrophin protein is not yet fully understood (for review see Hartzell et al., 2007). Recently, bestrophins have been found to comprise a new family of $Cl^-$ channels, some of which are activated by intracellular $Ca^{2+}$ (Sun et al., 2002; Qu et al., 2003, 2006b; Tsunenari et al., 2003; Chien et al., 2006). It remains unclear, however, whether defects in bestrophin $Cl^-$ channel function are capable of completely explaining the diseases (Marmorstein et al., 2006; Yu et al., 2006, 2007; Hartzell et al., 2007). Some investigators have shown that another function of bestrophin is to regulate $Ca^{2+}$ signaling (Rosenthal et al., 2005; Marmorstein et al., 2006).

In addition to being activated by intracellular $Ca^{2+}$, hBest1 and mBest2 are also sensitive to differences in osmotic pressure across the plasma membrane (Fischmeister and Hartzell, 2005). A 20% increase in extracellular osmolality almost completely inhibits hBest1 or mBest2 currents expressed in HEK cells. The decrease in current is paralleled by a decrease in cell volume. Conversely, decreases in extracellular osmolality increase current, but the effect of hyposmolality is difficult to interpret because an endogenous swelling-activated current is present in HEK cells. Nevertheless, these results raise the possibility that bestrophins are volume-regulated anion channels (VRACs).

VRACs play a central role in homeostasis of cell volume by the process of regulatory volume decrease (RVD). When cells swell in response to an osmotic gradient across the plasma membrane, VRACs, $K^+$ channels, and various transporters are turned on (Hoffmann and Simonsen, 1989; Nilius et al., 1997; Lang et al., 1998). Although the exact complement of channels and transporters depends on cell type, efflux of ions from the cell is followed by water and the cells return to their normal cell volume. The molecular identity of the VRAC current has been elusive with at least six different candidates having been proposed (Nilius et al., 1997; Eggermont et al., 2001; de Tassigny et al., 2003).

Correspondence to Criss Hartzell: criss.hartzell@emory.edu

Abbreviations used in this paper: CaCC, calcium-activated Cl channel; dBest, *Drosophila* bestrophin; hBest, human bestrophin; RPE, retinal pigment epithelium; RVD, regulatory volume decrease; VRAC, volume-regulated anion channel.

To investigate if bestrophins could possibly be VRACs, we used *Drosophila* S2 cells as a model system. Using RNAi, we have previously shown that endogenous bestrophins are responsible for $Ca^{2+}$-activated $Cl^-$ channels (CaCCs) in S2 cells (Chien et al., 2006). Here we show that bestrophin currents in S2 cells are sensitive to osmotic pressure and that knockdown of dBest1 expression abolishes volume-regulated $Cl^-$ currents and significantly reduces RVD. The volume-regulated current does not require $Ca^{2+}$. These data show that dBest1 is independently activated by $Ca^{2+}$ and by cell swelling and is a member of the VRAC family that mediates RVD.

## MATERIALS AND METHODS

### Cell Culture

*Drosophila* S2 cells were cultured as described previously at room temperature (22–24°C) in Schneider's *Drosophila* Medium (GIBCO BRL) with 10% heat-inactivated FBS (GIBCO BRL) and 50 U/ml penicillin and 50 μg/ml streptomycin (GIBCO BRL) (Chien et al., 2006). S2 cells were seeded at a density of $\sim 10^6$ cells/ml in 10-cm Petri dishes and were split 1:4 weekly.

### Solutions

Unless indicated otherwise, the standard extracellular solution (E300) used for patch clamping S2 cells contained (in mM) 115 NaCl, 2 $CaCl_2$, 1 $MgCl_2$, 5 KCl, 10 HEPES (pH 7.2 with NaOH), and 48 mannitol to achieve 300 mosmol $kg^{-1}$. The intracellular solution (I300) contained (in mM) 110 CsCl, 10 EGTA (nominally 0 $Ca^{2+}$) or Ca-EGTA (high Ca), 8 $MgCl_2$, 10 HEPES (pH 7.2), and 45 mannitol to achieve 300 mosmol $kg^{-1}$. Osmotic pressure differences are expressed as Δmosmol $kg^{-1}$ (osmolality inside − osmolality outside). The Ca-EGTA stock solution was made by mixing 95 mM $CaCO_3$ and 100 mM EGTA at pH 7.0 (adjusted with CsOH) and titrating the final [$Ca^{2+}$] to make it equal to [EGTA] by the pH-metric method (Tsien and Pozzan, 1989). The free measured $Ca^{2+}$ concentration in the high $Ca^{2+}$ solution was typically ~4.5 μM. Intracellular solutions of other osmolalities (such as I320 and I340) were prepared by adding mannitol to this I300 solution until the desired osmolality was achieved. For nominally 0 Ca conditions, $CaCl_2$ in the E300 solution was replaced with 2 mM $MgCl_2$ and 1 mM EGTA was added. In addition, 5 mM BAPTA was added to the I300 solution before adjusting the osmolarity to 320 mosmol $kg^{-1}$ with mannitol. *Drosophila* saline contained (in mM) 117.5 NaCl, 20 KCl, 2 $CaCl_2$, 8.5 $MgCl_2$, 20 glucose, 10.2 $NaHCO_3$, 4.3 $NaH_2PO_4$, and 8.6 HEPES, pH 7.4 (330 mosmol/kg).

### RNA Interference

Double-stranded RNA was synthesized using the Ambion Mega-script High-Yield Transcription Kit RNA. 40 μg of *Drosophila* bestrophin subtype-specific double-stranded interfering RNA was applied to S2 cells in serum-free medium for 30 min at room temperature. Cells were patch clamped 6 d after RNAi treatment. We have previously described some of the *Drosophila* bestrophin RNAi constructs that are used here (Chien et al., 2006), but all of the constructs are described in Table I. The control RNAi was double-stranded RNA from a mammalian intron. Possible off-target effects of each RNAi were evaluated by BLASTing the RNAi sequence against the *Drosophila* genome. Off-target hits >17 nucleotides in length are listed in Table I.

### RT-PCR

The efficiency of gene silencing by RNAi was evaluated by reverse transcriptase PCR (RT-PCR). Total RNA was purified by the Trizol (Invitrogen) method. Bestrophin gene-specific primers were designed to span exon/exon boundaries to ensure that genomic DNA was not amplified. Primers for RT-PCR were as follows: dBest1, 5′-TCGATGAAATGGCCGATGATG-3′ and 5′-ATGCTCTCCACTGTCTCTCG-3′; dBest2, 5′-CGCGGACTATGAAAGCGTGG-3′ and 5′-CTGGAATACTGCTCGGCGTG-3′; dBest3, 5′-GTAACAAGGGCTCGAAAGGAAGGT-3′ and 5′-CACGGCATATGGCAACTCAGC-3′; dBest4, 5′-GAGAGCGCGGAGGGAGAATAAAAT-3′ and 5′-CCGTGGAAGCTGCTGGAGGAT-3′; Act5C, 5′-TCAGCCAGCAGTCGTCTAATCCAG-3′ and 5′-GCGGGGCCTCGGTCAGC-3′. RT-PCR was conducted using SuperScript III One-Step RT-PCR with Platinum Taq (Invitrogen). PCR band densities were quantified using an AlphaImager Imaging System (Alpha Innotech). Each PCR band was excised, gel purified, and cloned into pCRII-TOPO (Invitrogen) for sequencing.

TABLE I

*Primers for Drosophila Bestrophin RNAi*

| RNAi | Primers | bp | Off-target genes |
|---|---|---|---|
| dB1C | GCAACGCCCAGTCAGGA | 793 | CG4623 (20/20) |
| | TCATCGTCGAATTGGAGAAC | | CG8831 (18/18) |
| | | | CG16711 (18/18) |
| dB1S | TGATGCCAGTGGCATTCAC | 509 | CG4623 (20/20) |
| | CGCCAGGTGGAAATAGGTT | | CG16711 (18/18) |
| dB1U3 | CCGCTGACATATACTGGACAT | 411 | Sif (19/19) |
| | ATTTGGCATTTCATTTTTATTT | | |
| dB1U5 | TGTTTGTCTAAGCCCTTCTACCTC | 206 | Indy (22/22) |
| | ATTGCTGTTCTTCTTTCCGACTGT | | CG33691 (23/24) |
| dB2C | CCAGCTCGGTCCTAATG | 798 | ninaE (18/18) |
| | CCTCTCCGGTCTTTTGTT | | |
| dB2S | AAACATCACCACTCTGTCGT | 503 | ninaE (18/18) |
| | TTGAGGGGGCCGAGGAT | | |
| dB2U3 | CATTGTGCCACCCAGAACC | 340 | CG14864 (21/22) |
| | GCAAGTGCCAAAACAATAAGTCA | | |
| dB2U5 | GAGCGCAGTTTGGTTGAGTTTGTC | 289 | Pncr004 (19/19) |
| | AAGGCCGAATTGTTGTTGTTTGAT | | |
| dB3N | GATCGGGATATTAAGCACTACA | 783 | CG8932 (21/22) |
| | GTCCTCCTCCTTTCTCTTTTTC | | |
| dB4N | TGGCCACGTACTCCTTCTTCCT | 784 | dBest1 (49/53) |
| | GCTCTGTCCCCCGCTTCCT | | |

Primers are listed 5′ to 3′ with the forward primer on top. T7 site (5′-CTAATACGACTCACTATAGGGAG-3′) was added to 5′ ends of all primers for in vitro RNAi synthesis. Off-target hits were identified by Blastn against the *Drosophila* genome. Numbers in parentheses indicate number of identical nucleotides within a stretch of x nucleotides. Only homologies >17 bp are shown. The Harvard *Drosophila* RNAi Screening Center has chosen 19-bp homology as the critical threshold for off-target effects (Kulkarni et al., 2006).

### Immunoblotting

Antibodies to dBest1 were raised in rabbits against amino acids 440–718 with $(His)_6$ tags (Chien et al., 2006). For Western blot, a crude membrane fraction of S2 cells was separated by SDS-PAGE on 10% Tris-HCl polyacrylamide gels and blotted to PDVF membrane. The antibody was used at 1:5,000 dilution and detected by enhanced chemiluminescence (Super Signal, Pierce Chemical Co.). The antibodies did not recognize a band in the dbest1 knockout fly.

### S2 Cell Transfection

The dBest1 open reading frame was PCR'd and introduced into KpnI (5′) and NotI (3′) sites of pAc5.1/V5-HisA *Drosophila* expression vector (Invitrogen). For the rescue experiment, a mixture of 2–4 μg of purified pAC5.1-dBest1ORF and 0.5–1 μg of pAC5.1-EGFP was used to transfect $4.2 \times 10^5$ S2 cells treated with dB1U5 RNAi for 4 d with calcium phosphate. Cells treated with dB1U5 RNAi and transfected with 2–4 μg of pAC5.1-EGFP were used as controls. Green cells were patch clamped 2–3 d after transfection.

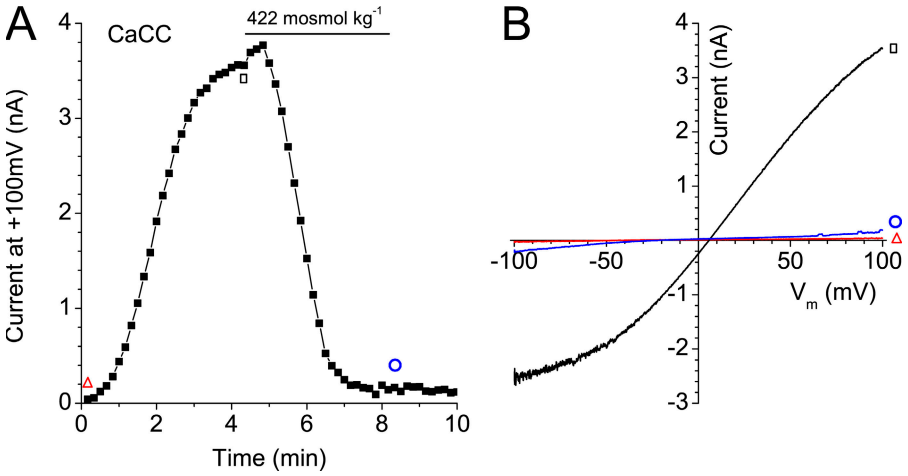


**Figure 1.** Native *Drosophila* S2 $Ca^{2+}$-activated $Cl^-$ currents are sensitive to osmotic pressure. (A) Time course of typical S2 endogenous $Ca^{2+}$-activated $Cl^-$ currents (CaCCs). Whole cell patch clamping was initiated in *Drosophila* S2 cells with isosmotic (320 mosmol $kg^{-1}$) intracellular (~4.5 μM free $Ca^{2+}$) and external solutions. Voltage ramps from −100 to +100 mV were given from a holding potential of 0 mV at 10-s intervals. After the CaCC had reached a plateau amplitude, the bath was replaced with a hyperosmotic external solution (422 mosmol $kg^{-1}$ by addition of mannitol). (B) Current–voltage relationship of the CaCC current measured at the beginning (open triangle), the plateau (open square), and after hyperosmotic shock (open circle). Internal solution (in mM) was 165 CsCl, 8 $MgCl_2$, 10 Ca-EGTA, 10 HEPES, pH 7.4. External solution: 150 NaCl, 1 MgCl2, 2 $CaCl_2$, 10 HEPES, pH 7.4, 20 mannitol (320 msomol $kg^{-1}$).

### Regulatory Volume Decrease

For monitoring RVD, day 6 RNAi-treated S2 cells were washed and allowed to equilibrate for 15 min in *Drosophila* saline. Cells that were round with a bright membrane were chosen for cell volume measurement. The average diameter of the selected cells was 15.5 ± 0.8 μm. Phase contrast images of the cells were taken at 5-s intervals and were analyzed with MetaMorph Imaging software (Universal Imaging Co.). The volume of the cell was calculated from the measured circumference assuming that the shape of S2 cells is spherical. After 1 min, the cells were exposed to hypo-osmotic saline (166 mosmol $kg^{-1}$), which was made by mixing equal amount of *Drosophila* saline with deionized $H_2O$. The imaging was continued for ~30 min before returning to isosmotic *Drosophila* saline. RVD was expressed as % recovery = $(Vol_{peak} - Vol_{30min})/Vol_{peak}$, where $Vol_{peak}$ is the maximum cell volume and $Vol_{30min}$ is the volume 30 min after switching to hyposmotic solution.

### Electrophysiology and Imaging

S2 cells were allowed to adhere to the bottom of the recording chamber for 10 min and were then washed and incubated with extracellular solution for 15 min before whole cell recording. All patch-clamp recordings were performed within the next 30 min. Fire polished pipettes pulled from borosilicate glass (Sutter Instrument Co.) had resistances of 2–3 MΩ when filled with intracellular solution. For whole-cell recording, cells were voltage clamped with ~1-s duration ramps from −100 to +100 mV run at 10-s intervals or 750-ms voltage steps from −100 mV to +100 mV in 20-mV increments (Chien et al., 2006). Whole cell recording data were filtered at 2–5 kHz and sampled at 5–10 kHz by an Axopatch 200A amplifier controlled by Clampex 8.2 via a Digidata 1322A data acquisition system (Axon Instruments Inc.). Data were not corrected for liquid junction potentials, which were calculated to be ~4 mV. Series resistance compensation was not routinely employed, but cells were discarded if the series resistance was >10 MΩ (typically 5 MΩ). The average capacitance of the S2 cells was 14.2 ± 0.4 ($n = 89$). Data were analyzed using pClamp 9 software and Origin 7.0 and are expressed as mean ± SEM.

## RESULTS

### $Ca^{2+}$-activated $Cl^-$ Currents Are Blocked by Extracellular Hyperosmolality

To determine whether native bestrophin currents in S2 cells are sensitive to osmolality, S2 cells were voltage clamped under isosmotic conditions with an intracellular solution that contained high $Ca^{2+}$ (~4.5 μM). The current was small (0.04 nA) immediately after patch break and then slowly activated with a half-time of 2.1 min to reach a plateau of 3.6 nA, as we have described previously (Fig. 1). We have previously concluded that this $Ca^{2+}$-activated current is mediated by dBest1 and possibly by dBest2 because it is abolished by RNAi to dBest1 or dBest2 (Chien et al., 2006). Increasing extracellular osmolality 30% caused a dramatic reduction of the current to 0.2 nA (Fig. 1). This effect of extracellular hyperosmotic solution was similar to that described for hBest1 and mBest2 expressed in HEK cells (Fischmeister and Hartzell, 2005). When the extracellular solution was returned to isosmotic, the current usually increased very slowly and did not return to the initial current amplitude even after ~5 min. We observed a similar sluggish reversibility of mBest2 currents inhibited by hyperosmotic solutions (Fischmeister and Hartzell, 2005). We suspect that this relative irreversibility can be explained by the nonphysiological magnitude of the osmotic pressure changes resulting in disruption of the coupling between the volume sensor and the bestrophin current. Under our usual recording conditions (<5 min), the current does not run down in isosmotic conditions.

Bestrophin currents are activated by extracellular hyposmolality. To test whether bestrophin currents could be activated by osmotic pressure independently of $Ca^{2+}$, we measured $Cl^-$ currents in S2 cells voltage-clamped under anisosmotic conditions. S2 cells were allowed to adapt to the extracellular solution (E300) for 15 min before recording. The cells were then patch-clamped with nominally 0 $Ca^{2+}$ (<20 nM) intracellular solutions that were either isosmotic (I300) or hyperosmotic (I320, Δ20 mosmol $kg^{-1}$ or I340, Δ40 mosmol $kg^{-1}$). Fig. 2 A shows typical traces of osmotically activated $Cl^-$ currents recorded with voltage ramps at Δ20 mosmol $kg^{-1}$ osmotic pressure.

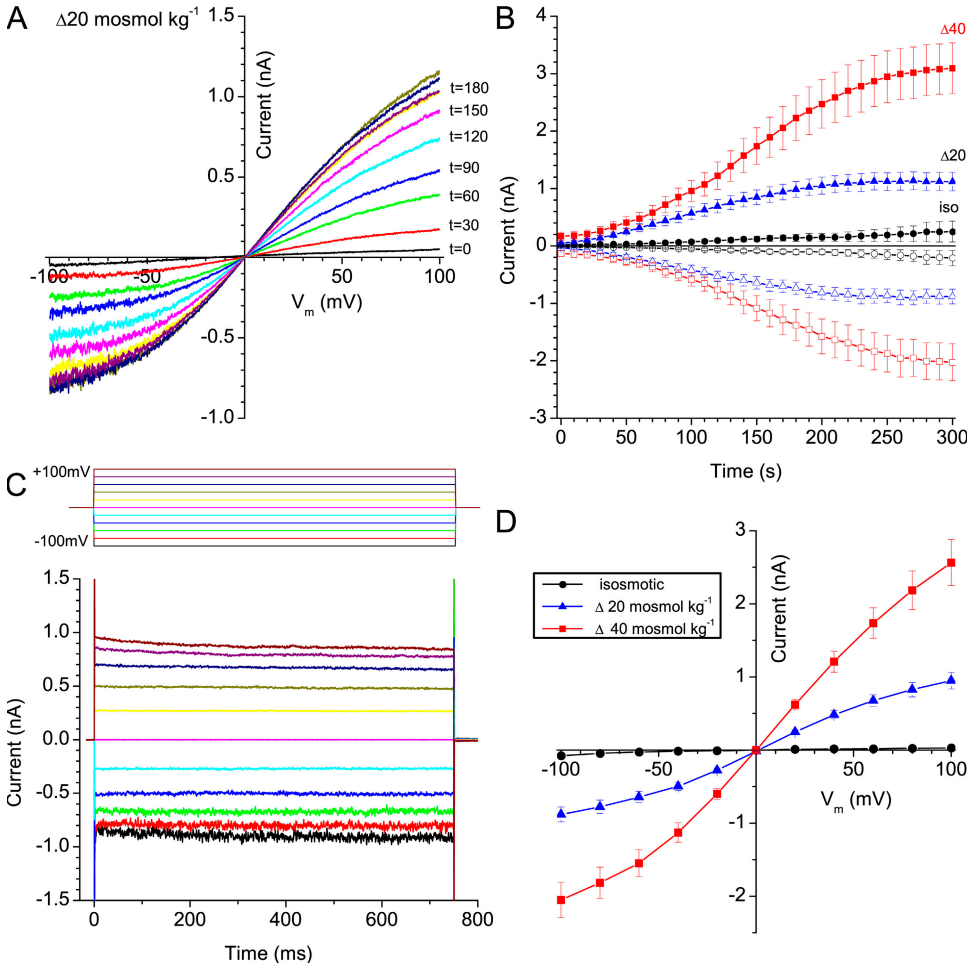


**Figure 2.** *Drosophila* S2 cells express endogenous osmotically activated $Cl^-$ currents. (A and B) Time-dependent activation of the osmotically activated $Cl^-$ currents in S2 cells. (A) Traces of a typical S2 osmotically activated $Cl^-$ current recorded by voltage ramps from −100 to +100 mV at 10-s intervals after establishing whole-cell recording with Δ20 mosmol $kg^{-1}$ (intracellular solution: nominally 0 $Ca^{2+}$ I320; external solution: E300). (B) Time course of the osmotically activated $Cl^-$ currents measured at −100 mV (open symbols) and +100 mV (solid symbols) at Δ40 mosmol $kg^{-1}$ (squares, $n = 9$), Δ20 mosmol $kg^{-1}$ (triangles, $n = 13$), and Δ0 mosmol $kg^{-1}$ (circles, $n = 6$). (C) Current traces of a typical osmotically activated (Δ20 mosmol $kg^{-1}$) $Cl^-$ current in response to voltage steps (20 mV intervals from −100 to +100 mV) after the ramp current had reached a peak (~4 min). (D) Steady-state current–voltage relationship with Δ40 mosmol $kg^{-1}$ ($n = 9$), Δ20 mosmol $kg^{-1}$ ($n = 16$), and Δ0 mosmol $kg^{-1}$ ($n = 5$). All averaged data are represented as mean ± SEM.

The time course of the development of the osmotically activated $Cl^-$ current is shown in Fig. 2 B. The initial whole cell current immediately after patch break was on average <0.1 nA regardless of the osmotic pressure. With isosmotic solutions, the current remained stable at <0.2 nA for >9 min after patch break ($n = 6$). In contrast, with an internal solution having a higher osmolality than the extracellular solution, the current ran up briskly with a mean half time of 2.4 ± 0.1 min ($n = 28$) before reaching a peak that was on average 45.1 ± 7.3-fold (Δ20 mosmol $kg^{-1}$, $n = 13$) or 60.1 ± 15.2-fold (Δ40 mosmol $kg^{-1}$, $n = 9$) greater than the initial current amplitude (Fig. 2 B). Voltage steps from −100 mV to +100 mV in 20-mV steps were applied to the cell after the ramp current had reached a peak value (~4 min, Fig. 2 C). $Cl^-$ currents activated by Δ20 or Δ40 mosmol $kg^{-1}$ did not show time-dependent activation or inactivation in response to voltage steps. Steady-state I-V curves showed a characteristic S shape (Fig. 2 D). The characteristics of the current activated by osmotic pressure are virtually identical to the current that we previously described as being activated by intracellular $Ca^{2+}$ (Chien et al., 2006). The I-V curves are identical: both are S shaped, the currents exhibit little time dependence, the currents reverse near $E_{Cl}$, and both the osmotically activated current and the $Ca^{2+}$-activated current have characteristic noise at negative potentials.

### Osmotically Activated Cl Currents Correlate with Cell Swelling

To determine whether activation of the bestrophin current was related to osmotically induced changes in cell volume, we imaged patch-clamped cells at intervals during a recording session. The time course of the development of a typical bestrophin $Cl^-$ current and cell volume change in response to Δ20 mosmol $kg^{-1}$ is shown in Fig. 3 A. Cell swelling preceded the activation of the $Cl^-$ current. Also, the magnitude of the current was related to cell volume. The cell volume and the current were larger with greater osmotic pressure differences (Fig. 3 B). At the peak of hyposmotic swelling, the cell volume increase was 50.3 ± 11.6% ($n = 4$) with Δ20 mosmol $kg^{-1}$ and 118.9 ± 38.8% ($n = 3$) with Δ40 mosmol $kg^{-1}$. Patch-clamped cells exposed to hyposmotic solutions should theoretically swell indefinitely and burst because the intracellular osmolality is effectively buffered by the patch pipet so that water influx can never equilibrate the osmolality (Ross et al., 1994). In our experiments, cells exposed to

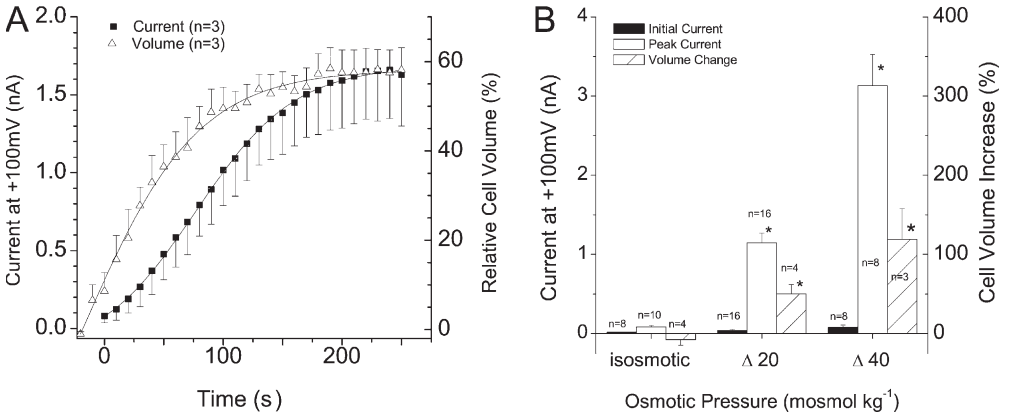


**Figure 3.** *Drosophila* S2 osmotically activated $Cl^-$ currents are correlated with cell swelling. (A) Time courses of the increase in cell volume (open triangles) and the Cl current amplitude after patch break at +100 mV (solid squares) with Δ20 mosmol $kg^{-1}$ ($n = 3$). The change in cell volume was calculated as a percentage of the cell volume ~30 s before patch break. The first data point shown is immediately after patch break. Current measurements were begun after cell capacitance and series resistance were measured, ~20 s after patch break. (B) Mean current amplitudes at +100 mV at the onset of whole cell recording (filled bars) and after the currents had reached a peak (open bars) and the corresponding cell volume increase (hatched bars) with Δ40 mosmol $kg^{-1}$, Δ20 mosmol $kg^{-1}$, and Δ0 mosmol $kg^{-1}$. Cell volume change is expressed as percent increase in cell volume from the initiation of whole cell recording to ~5 min after patch break when the currents had approached a steady value. For zero osmotic pressure, the cell volume change was measured 5 min after the initiation of whole cell recording. (mean ± SEM). *, significantly different from control at $P < 0.01$. Solutions were the same as used in Fig. 2.

Δ40 mosmol $kg^{-1}$ often burst eventually, but those exposed to Δ20 mosmol $kg^{-1}$ usually reach a terminal volume during the time course (<10 min) of our experiments. This has also been observed by other investigators, but the mechanisms remain unclear (Ross et al., 1994). Cells recorded in isosmotic solutions remained stable or decreased in volume a small amount (−7.7 ± 6.9%) ($n = 4$). The data in Figs. 1–3 suggest that the current activated by cell swelling is a member of the VRAC family.

### Osmotically Activated Current Is Mediated by dBest1

The osmotically activated $Cl^-$ currents share many characteristics with the CaCC currents described previously (Chien et al., 2006). (a) The currents activate slowly with time after patch break; (b) both currents are noisy at negative membrane potentials; (c) the currents in response to voltage steps are time independent; and (d) both currents have minor voltage dependence at voltage extremes so that the macroscopic currents recorded in response to voltage ramps are S shaped. These similarities suggest that osmotic pressure can activate the same current in the absence of intracellular $Ca^{2+}$ that is activated in isosmotic conditions by high intracellular $Ca^{2+}$. We have used RNAi to test if bestrophins mediate the osmotically activated $Cl^-$ current. S2 cells were treated with bestrophin subtype-specific RNAi or control dsRNA. Osmotically activated $Cl^-$ currents were measured 6 d later. Cells that were treated with control dsRNA developed currents of 1.07 ± 0.12 nA ($n = 25$) in response to Δ20 mosmol $kg^{-1}$ (I320, E300) osmotic pressure (Fig. 4 A, red bars). Four dBest1 RNAi constructs were designed. Two of these, dB1C and dB1S, were made to sequences coding for the C terminus of dBest1 and have previously been shown to abolish the CaCC currents in S2 cells (Chien et al., 2006). The other two (dB1U5 and dB1U3) were made to the 5′ and 3′ UTRs of dBest1, respectively. Three of these four RNAi constructs (dB1C, dB1S, and dB1U5) each abolished the osmotically activated current (Fig. 4 A). dB1U3 significantly reduced, but did not completely abolish, the osmotically activated current (Fig. 4 A). The fact that the current was abolished or significantly reduced with different RNAi constructs to dBest1 strongly suggests that dBest1 is a major player in the VRAC current in these cells. These four RNAi constructs against dBest1 also abolished, or greatly reduced, the CaCC currents (Fig. 4 B, open bars).

All four of the dBest1 RNAi constructs reduced dBest1 protein expression as judged by Western blot (Fig. 4 C) and RT-PCR (Fig. 4 D). In 22 separate RNAi transfections with these four constructs, dBest1 protein levels were abolished or barely detectable by Western blot (examples in Fig. 4 C). We did observe some "off-target" effects of some of the dBest1 RNAi constructs on other bestrophin transcripts. dB1C and dB1U5 reduced dBest2 in some experiments. We do not understand the mechanism of these effects. There is very little identity between dBest1 and dBest2 in the region defined by these RNAs (Table I), but other factors have been shown to be involved in off-target effects of RNAi (Jackson et al., 2006; Moffat et al., 2007; Rual et al., 2007; Svoboda, 2007).

To test the specificity further, we designed an experiment to rescue the dBest1 RNAi–treated cells. Cells were treated with dB1U5 RNAi for 4 d. The cells were then transfected with plasmid encoding either GFP alone or dBest1 plus GFP (Fig. 5). VRAC currents were measured in response to Δ20 mosmol $kg^{-1}$ (nominally 0 $Ca^{2+}$ I320, E300) osmotic pressure. CaCCs were measured in isosmotic conditions with ~4.5 μM free internal $Ca^{2+}$. dB1U5-treated cells transfected with GFP alone had virtually no VRAC or CaCC (Fig. 5, A, C, and F). In contrast, dB1U5-treated cells transfected with dBest1 had very large VRACs and CaCCs (Fig. 5, B, D, and F).

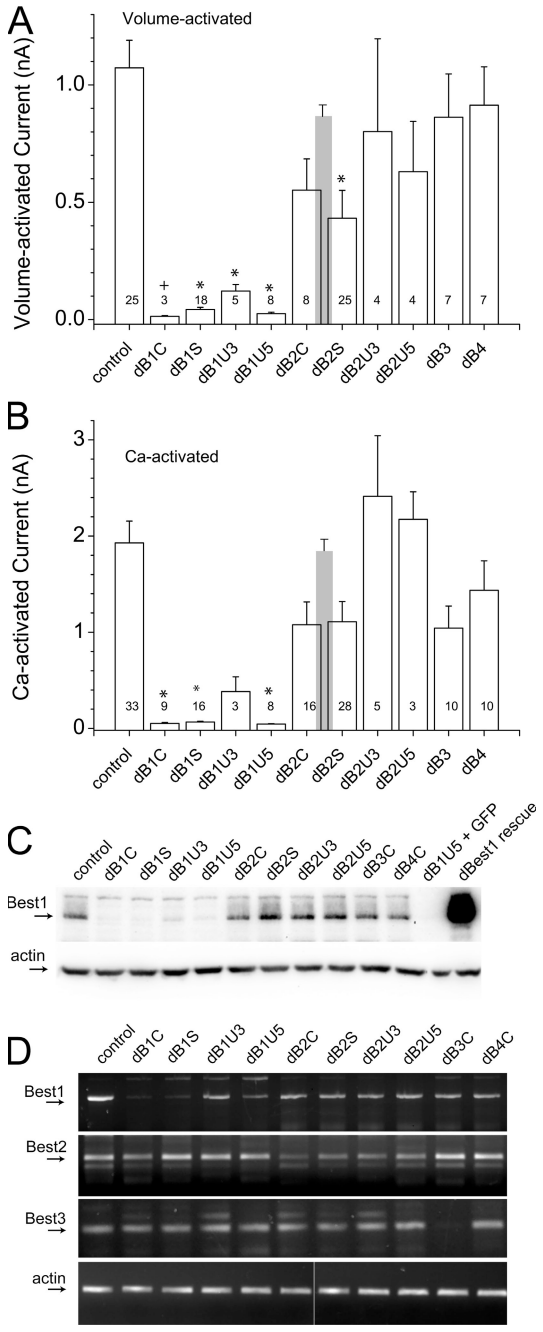


**Figure 4.** RNAi inhibition of the native S2 volume-activated $Cl^-$ currents. S2 cells were treated with control dsRNA (from a mammalian intron) or *Drosophila* bestrophin subtype-specific RNAi before patch clamping at day 6. Mean amplitudes of $Cl^-$ currents at +100 mV were measured for the (B) Ca-activated currents (~40 μM free $Ca^{2+}_i$, isosmotic solutions, open bars) and the (A) volume-regulated currents (E300, nominally 0 $Ca^{2+}_i$ I320, Δ20 mosmol $kg^{-1}$, red bars) after the currents had reached peak amplitude 4–5 min after patch break. (mean ± SEM). *, significantly different from control at $P < 0.01$. +, significantly different from control at $P < 0.02$. The gray bars show the mean current amplitudes of cells treated with dB2S or dB2C for which Western blot data were available to show that dBest1 protein levels were close to control. Some of the CaCC data for dB1S, dB1C, dB2C, dB2S, dB3C, and dB4C have previously been published (Chien et al., 2006). (C) Effects of RNAi on dBest1 protein expression. S2 cells treated 6 d earlier with the indicated RNAi constructs were extracted with SDS and the Western blot was probed with dBest1 antibody. (D) RT-PCR of bestrophin transcripts from S2 cells treated with different RNAi constructs. RT-PCR was performed using the primers described in Materials and methods. RNA was extracted 6 d after RNAi treatment for dBest1 and dBest2 and 2 d after RNAi treatment for dBest3. The actin gel was composited from two different gels that were run in parallel (lanes 1–6 are from one gel and 7–11 from the second). The white line indicates that intervening lanes have been spliced out.

Transfection with dBest1 resulted in a significant overexpression of dBest1 protein (Fig. 4 C). The currents exhibited the typical characteristics of the endogenous current: slow activation after patch break (Fig. 5 E), S-shaped I-V curve (Fig. 5, B and D), noisy currents at negative potentials (Fig. 5, B and D), and time-independent currents in response to voltage steps (not depicted). Although both the $Ca^{2+}$-activated and the osmotically activated currents turned on slowly after patch break, the rescued currents generally activated about twice as fast as the endogenous currents (Fig. 5 E, $\tau = 1$ min). This might be related to the high level of overexpression of dBest1.

### Effects of dBest2 RNAi

Four dBest2 RNAi constructs were made, two to sequences coding for parts of the C terminus of dBest2 (dB2C and dB2S), one to part of the 5′-UTR (dB2U5), and one to part of the 3′-UTR (dB2U3). dB2U3 and dB2U5 reduced dBest2 message levels, but had no significant effect on the VRAC or CaCC current (Fig. 4, A, B, and D). dB2C and dB2S reduced both CaCC and VRAC currents ~50%, but the effects were not statistically significant (at either the 0.05 or 0.01 level), except for the effect of dB2S on the VRAC current (Fig. 4 A). The current decreases caused by dB2C and dB2S can be explained by a variable off-target effect of these RNAi constructs on dBest1. In 4 out of 13 different RNAi transfections with the dB2C and dB2S constructs, dBest1 protein levels were reduced to <10% of the control level. In six separate experiments where dBest1 protein was apparently the same as control, mean current amplitudes in dB2C- and dB2S- treated cells were identical to control (CaCC: 1.84 ± 0.19 nA, $n = 23$, VRAC: 0.75 ± 0.16 nA, $n = 10$, gray bars in Fig. 4, A and B) We do not understand the variability or the mechanism of this off-target effect. There is very little identity between dBest1 and dBest2 in the region comprising the RNAi. The largest cluster of matching bases was 14 with 3 mismatches, which should not support RNA interference. In any case, these results support the idea that both the VRAC and CaCC currents are mediated by dBest1 and that dBest2 is not necessary. Previously, we reported that dB2C and dB2S abolished CaCC currents in S2 cells (Chien et al., 2006). However, we now believe that this is explained by an off-target effect of these two RNAi constructs on dBest1.

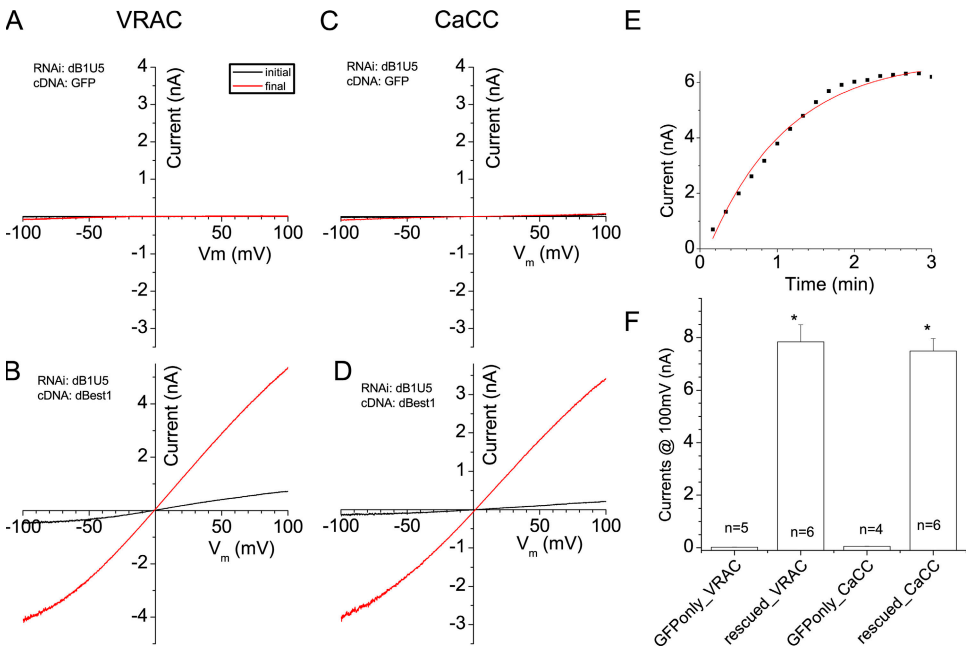


**Figure 5.** Rescue of Ca-activated and volume-regulated currents. Cells were treated with dB1U5 RNAi for ~4 d and then transfected with either GFP alone (A and C) or GFP + dBest1 (B and D) and recorded 18–24 h later. (A–D) Typical I-V curves for VRAC (A and B) and CaCC (C and D) immediately after patch break (black) and after the current had reached maximum (red, ~2–4 min after patch break). (A and B) VRACs were recorded with nominally 0 $Ca^{2+}$ internal solution (I320) and E300 extracellular solution. (C and D) CaCCs were recorded with ~4.5 μM internal free Ca and isosmotic (300 mosmol $kg^{-1}$) solutions. (E) Time course of activation of VRAC current after patch break of a typical dBest1-rescued cell. (F) Average amplitude (mean ± SEM) of currents at +100 mV ~4–5 min after patch break corresponding to the conditions in A–D. *, significantly different from GFP alone, $P < 0.01$.

### Effects of RNAi against dBest3 or dBest4

dB3C was quite specific and effective in reducing dBest3 mRNA (Fig. 4 D), but had no effect on either the CaCC or VRAC currents (Fig. 4, A and B). Thus, we can eliminate dBest3 as a contributor to these currents. Our experiments with dBest4, however, have been inconclusive. Although dB4C consistently had no effect on CaCC or VRAC currents, dBest4 expression varied from culture to culture so that the effect of RNAi on dBest4 expression was difficult to evaluate, as we mentioned previously (Chien et al., 2006).

### Regulatory Volume Decrease Is Mediated by dBest1

To determine whether bestrophins play a role in RVD, we compared RVD in control cells and cells treated with bestrophin-specific RNAi. To measure RVD, S2 cells were first allowed to equilibrate in *Drosophila* saline for 15 min before the bath was replaced with hypo-osmotic saline. Control S2 cells exhibited robust RVD under these conditions (Fig. 6). In cells treated with control dsRNA, the hyposmotic solution caused the cells to swell to ~150% of their initial volumes within 1–2 min. The volume then decreased over a period of 30 min with an average recovery of ~75%. When the cells were returned to isosmotic solution, the cells shrank to a volume ~20% less than their initial volume in isosmotic solution. This is consistent with the decrease in volume in hyposmotic solution being due to RVD. Cells treated with RNAi to dBest3 or dBest4 had the same magnitude and time course of swelling and RVD as controls. In contrast, cells treated with dBest1 RNAi (dB1S, dB1C, dB1U5) swelled to a larger extent and had a much slower time course of RVD (Fig. 6). The greater swelling in cells lacking dBest1 can be explained by the fact that control cells begin to regulate their volume even while they are swelling. Upon returning to isosmotic solution, the cell volume returned to a value close to the initial volume but did not decrease below this level, consistent with the absence of RVD.

### Activation of the Bestrophin Current Does Not Require $Ca^{2+}$

Although Fig. 2 suggests that activation of bestrophin currents can occur in the absence of intracellular $Ca^{2+}$, the bath solution in these experiments contained $Ca^{2+}$, so we cannot rule out the possibility that local $Ca^{2+}$ influx might activate the $Cl^-$ current. To test more rigorously whether the volume-regulated bestrophin current required $Ca^{2+}$ for activation, $Ca^{2+}$ was removed from all solutions and $Ca^{2+}$ chelators were added to both intra- and extracellular solutions. $CaCl_2$ in the E300 extracellular solution was replaced with 2 mM $MgCl_2$ and 1 mM EGTA was added to chelate residual free $Ca^{2+}$. Furthermore, 5 mM BAPTA was added to the intracellular solution. With Δ20 mosmol $kg^{-1}$ and nominally 0 $Ca^{2+}$ inside and out, the bestrophin current activated with approximately the same time course ($t/2 = 1.6 \pm 0.2$ min) as in control cells with $Ca^{2+}$ in the bath (2.3 ± 0.1 min), but the peak amplitude of the volume-activated Cl currents in nominally 0 $Ca^{2+}$ conditions was significantly smaller (0.36 ± 0.07 nA) than in controls (1.14 ± 0.12 nA) (Fig. 7).

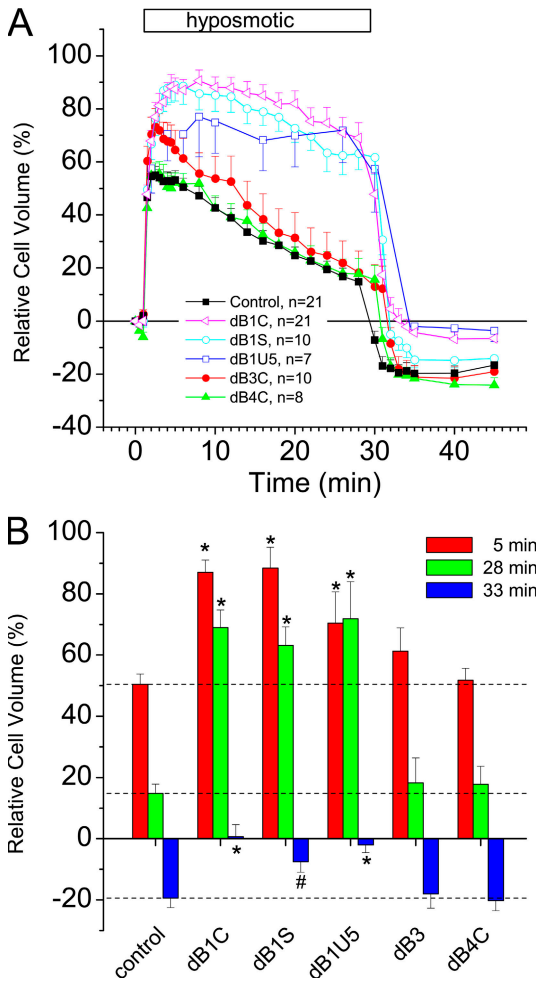


**Figure 6.** Regulatory volume decrease is inhibited by knockdown of dBest1. S2 cells were treated with RNAi specific to each *Drosophila* bestrophin subtype as described in Materials and methods for 6 d before quantification of RVD. RNAi-treated cells were pre-incubated in *Drosophila* saline (330 mosmol $kg^{-1}$) for 15 min before imaging. The *Drosophila* saline was replaced by a diluted solution of the same saline (1:1 with $H_2O$, 166 mosmol $kg^{-1}$) 1 min after the initiation of imaging. Cells were monitored by time lapse imaging for 30 min and cell volume was quantified with MetaMorph as described in Materials and methods. (A) Time course of increase in cell volume. Cell volumes were normalized to the initial volume and the time course of increase in cell volume (%) plotted as mean ± SEM. (B) Mean cell volume increase (%) near peak of cell swelling (red bars, ~4 min in hyposmotic solution), at the end of RVD (green bars, ~27 min in hyposmotic solution), and ~3 min after returning to isomotic solution (blue bars). *, significantly different from control at $P < 0.01$; #, significantly different from control at $P < 0.05$.

This result suggests that although $Ca^{2+}$ is not required for activation of the current by cell swelling, $Ca^{2+}$ is facilitatory. This finding is consistent with reports that VRAC is not activated by raising $[Ca^{2+}]_i$ (Hazama and Okada, 1988; Doroshenko and Neher, 1992) but may require a basal level of $[Ca^{2+}]_i$ for full activation (McCarty and O'Neil, 1992; Szucs et al., 1996; Nilius et al., 1997; Altamirano et al., 1998).

### Activation of Bestrophin by $Ca^{2+}$ Is Not Correlated with Cell Swelling

Although $Ca^{2+}$ is not required for the activation of swelling-activated bestrophin currents, we wanted to test whether high intracellular $Ca^{2+}$ stimulated current by inducing cell swelling. Bestrophin currents were activated by patch clamping under isosmotic conditions with high intracellular $Ca^{2+}$ and cell volume was measured. Cells recorded with high-$Ca^{2+}_i$ solution (4.5 μM) exhibited typical $Ca^{2+}$-regulated bestrophin currents that were small initially (0.12 ± 0.03 nA) and slowly developed to a plateau value of 2.48 ± 0.38 nA with a mean half time of 2.5 ± 0.2 min (Fig. 8 A). The corresponding cell volume in the same cells is shown in Fig. 8 B. Cell volume was normalized to the initial volume at the initiation of whole cell recording. Cell volume recorded with high intracellular $Ca^{2+}$ did not change during the recording. This result excludes the involvement of swelling in $Ca^{2+}$-dependent activation of bestrophin current and indicates that volume and $Ca^{2+}$ are parallel pathways regulating bestrophin currents. One caveat that must be considered, however, is that the sensitivity of our cell volume measurements may be limited such that small changes in cell volume that escape detection could possibly activate current.

When cells were patched with nominally 0 $Ca^{2+}$ intracellular (<20 nM) solution under isosmotic conditions, both initial and steady-state currents were <0.2 nA. While half of the cells had currents <0.2 nA throughout the recording (~5 min), the other half increased transiently to 0.47 ± 0.06 nA with a half time of 1.4 ± 0.2 min. The currents then declined and stabilized at <0.2 nA. The cell volume in all cells patched with nominally 0 $Ca^{2+}$ solution decreased gradually during the recording regardless of whether currents were activated transiently. The development of the transient current in nominally 0 $Ca^{2+}$ cells might be an effect of a transient $Ca^{2+}$ increase when whole cell patch clamp was initiated. The cells are patch clamped at a holding potential of 0 mV. If intracellular $Ca^{2+}$ increased as a result of the mechanical forces imposed by the patch pipet, the resulting $Ca^{2+}$ influx may not be immediately buffered by EGTA, which diffuses slowly from the pipet into the cell. In any case, we conclude that volume is not a factor causing the activation of $Ca^{2+}$-regulated bestrophin currents. Cell volume and $Ca^{2+}$ are two distinct mechanisms that regulate bestrophin current but they may not necessarily be mutually exclusive.

## DISCUSSION

### dBest1 Is a VRAC

Our results suggest that bestrophins are a kind of VRAC that is involved in cell volume control. The data supporting this suggestion include the following: (a) hyposmotic

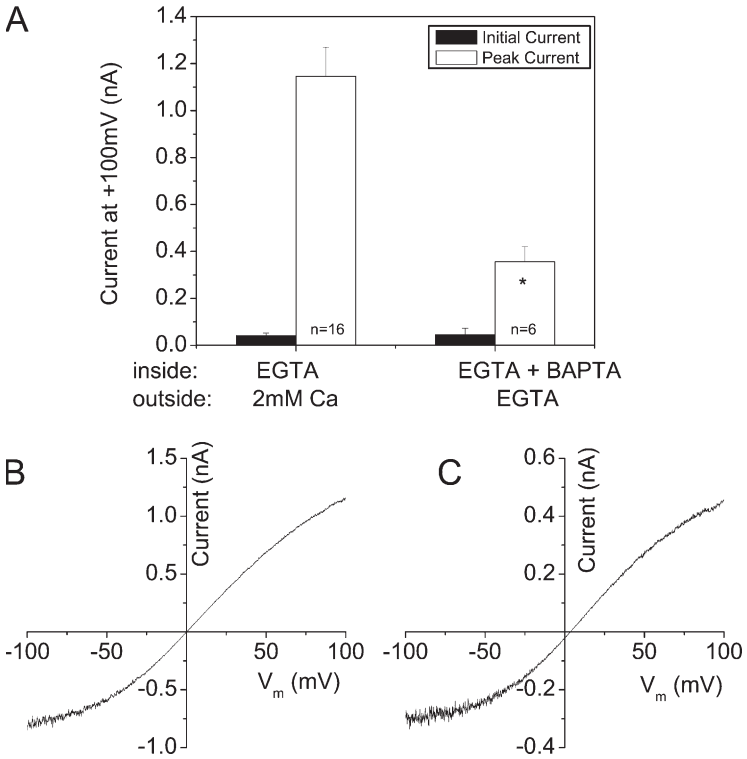


**Figure 7.** Volume-activated $Cl^-$ currents are $Ca^{2+}$ independent. (A) Average amplitudes of S2 volume-activated $Cl^-$ currents at +100 mV at the onset of whole cell recording (filled bars) and after the currents had reached peak values (open bars) with Δ20 mosmol $kg^{-1}$. Bars on the left were recorded in the normal solutions with 2 mM extracellular $Ca^{2+}$ (E300) and 10 mM intracellular EGTA (I320). Cells on the right were recorded with I320 intracellular solution with 5 mM BAPTA added and a nominally 0 $Ca^{2+}$ extracellular solution prepared by substituting external $Ca^{2+}$ with equimolar of $Mg^{2+}$ and adding 1 mM EGTA. *, significantly different from control at $P < 0.01$. (B) I-V curve from a voltage ramp for current corresponding to the left bars in A. (C) I-V curve for current corresponding to right bars in A.

cell swelling precedes activation of the osmotically sensitive $Cl^-$ current in S2 cells, (b) the osmotically sensitive current is abolished or greatly reduced by RNAi treatments that reduce dBest1 protein levels, (c) the inhibition of the current by RNAi can be rescued by overexpression of dBest1, (d) cells with reduced dBest1 expression have an impaired ability to regulate their cell volume in response to hyposmotic stress, and (e) there is an excellent correlation between the VRAC current and the ability of cells to undergo RVD.

The VRAC current is apparently mediated by the same channels that mediate the CaCC current, because the same RNAi treatments reduce both currents. Although a role for dBest1 in mediating both VRAC and CaCC is strongly supported by our data, other bestrophins do not seem to be involved. There is a discrepancy between our present results and those we recently published regarding the role of dBest2 in CaCC currents (Chien et al., 2006). Previously, we found that the CaCC current was suppressed by RNAi to either dBest1 or dBest2 and proposed that the CaCC current was comprised of a heteromer of dBest1 and dBest2. However, at that time, we did not carefully examine possible off-target effects of dBest2 RNAi on dBest1 expression. Here, we find that the dBest2 RNAi constructs made to ORF sequences sometimes reduce dBest1 expression. Thus, the simplest explanation of these results is that the effect of dBest2 RNAi is caused by a variable off-target effect on dBest1. This conclusion is also consistent with our observation (Chien et al., 2006) that dBest1 expressed in HEK cells recapitulates the endogenous S2 CaCC current in the absence of dBest2. The off-target effects cannot be explained simply by homology between dBest1 and dBest2; there is insufficient identity between the dBest2 and dBest1 RNAi's. It seems that there may be some coregulation of bestrophin expression.

### Similarities and Differences between Classical VRAC and S2 VRAC

The canonical VRAC current is outwardly rectifying, inactivates at positive potentials in a time-dependent manner, and is stimulated by different maneuvers including hyposmotic swelling, membrane stretching, inflation by positive pressure, shear stress, reduction of intracellular ionic strength, and application of GTPγS (Nilius et al., 1997). VRAC exhibits an anion selectivity of $SCN^- > I^- > NO3^- > Br^- > Cl^-$ > gluconate (Nilius et al., 1997). Bestrophins have a very similar anionic selectivity (Qu et al., 2006b). On the other hand, *Drosophila* bestrophin currents exhibit relatively little rectification and inactivate only slightly at positive potentials, unlike many VRACs, which outwardly rectify and inactivate at positive potentials. However, VRAC rectification and inactivation seems to depend on the recording conditions and cell type (Nilius et al., 1997; de Tassigny et al., 2003). For example, in endothelial cells, parotid acinar cells, T-lymphocytes, neutrophils, and skate hepatocytes, inactivation is small or even completely absent. Because VRACs are ubiquitously expressed, one might expect that bestrophins would also be ubiquitously expressed. Although the expression pattern of bestrophins has not yet been thoroughly characterized (Hartzell et al., 2007), it appears

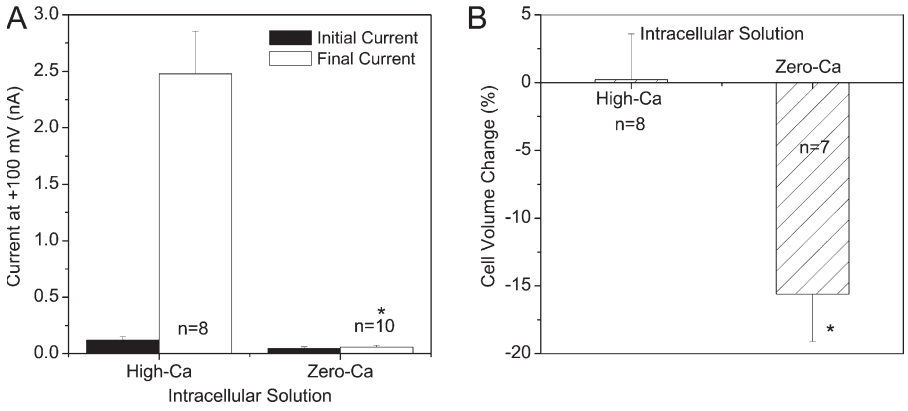


**Figure 8.** The S2 Ca-activated Cl current is not correlated with cell swelling. (A) Mean current amplitudes at +100 mV at the onset of whole cell recording (filled bars) and after the currents had reached steady states (open bars) in cells recorded with high intracellular $Ca^{2+}$ solution (4.5 μM) or nominally $Ca^{2+}$-free (<20 nM) intracellular solution. (B) Changes in cell volume (%) after the currents had reached steady state in cells recorded with high intracellular $Ca^{2+}$ solution (4.5 μM) or nominally $Ca^{2+}$-free (<20 nM) intracellular solution. Cell volumes were normalized to the basal cell volume measured at the initiation of the whole cell patch clamping. The data are represented as mean ± SEM. *, significantly different from high $Ca^{2+}$ at $P < 0.01$.

that their expression pattern is more restricted than that of VRAC. This would suggest that bestrophins may comprise only a subset of VRACs.

The single channel conductance of VRACs has been estimated to be ∼2 pS in endothelial cells, neutrophils, chromaffin cells, and T cells by stationary noise analysis (Nilius et al., 1997). This conductance is similar to what we have found for dBest1 channels (Chien et al., 2006). However, Jackson and Strange (1996) have questioned whether stationary noise analysis gives a reliable estimate of the VRAC conductance. They measured a single channel conductance of 15–50 pS (depending on membrane potential) by single channel recording and nonstationary noise analysis in C6 glioma cells and showed that stationary noise analysis underestimates the conductance by at least 10-fold. However, the gating of the $Ca^{2+}$-activated dBest1 channels in excised patches that we have described is complex; we often see what appears to be coordinated opening of several 2-pS events (Chien et al., 2006). The possibility exists that the 2-pS channels are substates and that physiological activation by changes in cell volume in intact cells may gate the channel differently than $Ca^{2+}$ does in excised patches.

Our results extend our previous findings that mBest2 and hBest1 in HEK cells exhibit sensitivity to cell volume (Fischmeister and Hartzell, 2005). In that paper, we were very cautious in equating bestrophins with VRACs for several reasons. Several molecules have been proposed to be VRACs (P-glycoprotein or Mdr, pICln, phospholemman, ClC-2, and ClC-3) but none has received wide acceptance (Nilius et al., 1997; Jentsch et al., 2002; de Tassigny et al., 2003). Because VRACs are ubiquitously expressed, it seems likely that these candidate proteins somehow regulate the expression or function of endogenous VRAC channels. This makes it very difficult to arrive at a molecular identification of VRAC in model cell lines such as HEK cells where endogenous VRAC is expressed. Our RNAi results here give us more confidence to propose that bestrophins are a kind of VRAC, but we remain highly circumspect.

Bestrophin VRAC currents in S2 cells are activated independently of $Ca^{2+}$. This is consistent with previous reports that the activation of VRAC does not require an increase of intracellular $Ca^{2+}$ (Hazama and Okada, 1988; Doroshenko and Neher, 1992). However, there is considerable evidence that although elevation of $Ca^{2+}$ is not necessary, a low level of $Ca^{2+}$ (∼50–100 nM) is required for VRAC activation, at least in certain cell types (Szucs et al., 1996; Nilius et al., 1997; Altamirano et al., 1998; Chen et al., 2007; Park et al., 2007). hBest1 has an $EC_{50}$ for $Ca^{2+}$ of ∼150 nM, which is very close to the permissive level for VRAC activation. Also, increases in cell volume are often accompanied by increases in intracellular $Ca^{2+}$ (McCarty and O'Neil, 1992).

Conversely, it seems that $Ca^{2+}$ can activate the current in the absence of cell volume changes. These data indicate that cell volume and $Ca^{2+}$ may be independent regulatory activators to bestrophin. It remains to be seen whether these two activators are truly independent or whether they converge on some common regulatory pathway.

### Implications for Best Disease

The finding that bestrophins may be VRACs suggests new hypotheses for the mechanisms of Best disease. hBest1 is located in the basolateral membrane of the retinal pigment epithelium (RPE) (Marmorstein et al., 2000). We have previously reported that mouse RPE cells exhibit a swelling-activated current that in many respects resembles bestrophin currents (Fischmeister and Hartzell, 2005) and other investigators have shown that RPE cells possess the appropriate ion channel and transport machinery to regulate cell volume (la Cour and Zeuthen, 1993; Civan et al., 1994; Kennedy, 1994; Adorante, 1995). The RPE is subject to conditions that would induce deviations in RPE volume as well as controlling the fluid composition of the space surrounding photoreceptors

(Gallemore et al., 1997; Fischmeister and Hartzell, 2005). Therefore, it is intriguing to speculate that at least part of the pathogenesis of Best disease and other bestrophin-linked retinal degenerative disorders might involve altered RPE cell volume regulation (Hartzell et al., 2007). There are several possible scenarios for the role of hBest1. hBest1 could simply be involved in adjusting RPE cell volume in response to changes in the composition of the fluid surrounding the photoreceptors. But, more likely, bestrophins are playing more subtle functions. VRACs have been implicated in a variety of other processes independent of cell swelling (Nilius et al., 1997; Eggermont et al., 2001). For example, hBest1 channels could be involved in regulating phagocytosis of photoreceptor outer segments. There is accumulating evidence that $Cl^-$ channels are involved in cell migration and cell shape changes in a variety of cell types (Kim et al., 2004; Day et al., 2006; Moreland et al., 2006). Also, $Cl^-$ channels including VRACs have been shown to play a role in regulation of cell pH (Nilius et al., 1997). Clearly, cells like RPE that have a large acidic lysosomal compartment need powerful mechanisms to handle protons. Obviously, the precise role played by these channels is purely speculative at this point in time, but the realization that they are sensitive to cell volume provides a platform for testable hypotheses.

Recently, it has been reported that knockout of Best1 in mouse has no effect on the CaCC currents in RPE cells where mBest1 is expressed (Marmorstein et al., 2000, 2006). This result certainly challenges the hypothesis that CaCC currents are mediated by Best1. However, although hBest1, mBest2, and dBest1 show $Ca^{2+}$ dependence under isosmotic conditions, it remains unclear whether all bestrophins have $Ca^{2+}$ dependence. For example, mBest3 does not appear to require $Ca^{2+}$ for activation (Qu et al., 2006a). The results presented here raise the possibility that mBest1 is not responsible for classical CaCC currents in RPE, but rather may be regulated by cell volume.

We thank all the members of the Hartzell lab, especially Yuan-yuan Cui, Sean Qu, Qinghuan Xiao, Carl Ying, and Kuai Yu for their assistance and support in this project, and Dr. Ken Moberg and his lab for help with *Drosophila* matters.

This work was supported by National Institutes of Health grants GM60448 and EY014852 and the American Health Assistance Foundation.

David C. Gadsby served as editor.

Submitted: 30 March 2007
Accepted: 4 October 2007

## REFERENCES

Adorante, J.S. 1995. Regulatory volume decrease in frog retinal pigment epithelium. *Am. J. Physiol.* 268:C89–C100.

Allikmets, R., J.M. Seddon, P.S. Bernstein, A. Hutchinson, A. Atkinson, S. Sharma, B. Gerrard, W. Li, M.L. Metzker, C. Wadelius, et al. 1999. Evaluation of the Best disease gene in patients with age-related macular degeneration and other maculopathies. *Hum. Genet.* 104:449–453.

Altamirano, J., M.S. Brodwick, and F.J. Alvarez-Leefmans. 1998. Regulatory volume decrease and intracellular $Ca^{2+}$ in murine neuroblastoma cells studied with fluorescent probes. *J. Gen. Physiol.* 112:145–160.

Chen, B., G. Nicol, and W.K. Cho. 2007. Role of calcium in volume-activated chloride currents in a mouse cholangiocyte cell line. *J. Membr. Biol.* 215:1–13.

Chien, L.T., Z.R. Zhang, and H.C. Hartzell. 2006. Single $Cl^-$ channels activated by $Ca^{2+}$ in *Drosophila* S2 cells are mediated by bestrophins. *J. Gen. Physiol.* 128:247–259.

Civan, M.M., C.W. Marano, F.W. Matschinsky, and K. Peterson-Yantorno. 1994. Prolonged incubation with elevated glucose inhibits the regulatory response to shrinkage of cultured human retinal pigment epithelial cells. *J. Membr. Biol.* 139:1–13.

Day, R.M., A.S. Agyeman, M.J. Segel, R.D. Chevere, J.M. Angelosanto, Y.J. Suzuki, and B.L. Fanburg. 2006. Serotonin induces pulmonary artery smooth muscle cell migration. *Biochem. Pharmacol.* 71:386–397.

de Tassigny, A.d., R. Souktani, B. Ghaleh, P. Henry, and A. Berdeaux. 2003. Structure and pharmacology of swelling-sensitive chloride channels, $I_{Cl,swell}$. *Fundam. Clin. Pharmacol.* 17:539–553.

Doroshenko, P., and E. Neher. 1992. Volume-sensitive chloride conductance in bovine chromaffin cell membrane. *J. Physiol.* 449:197–218.

Eggermont, J., D. Trouet, I. Carton, and B. Nilius. 2001. Cellular function and control of volume-regulated anion channels. *Cell Biochem. Biophys.* 35:263–274.

Fischmeister, R., and C. Hartzell. 2005. Volume sensitivity of the bestrophin family of chloride channels. *J. Physiol.* 562:477–491.

Gallemore, R.P., B.A. Hughes, and S.S. Miller. 1997. Retinal pigment epithelial transport mechanisms and their contributions to the electroretinogram. *Prog. Retinal Eye Res.* 16:509–566.

Hartzell, H.C., Z. Qu, K. Yu, Q. Xiao, and L.-T. Chien. 2007. Molecular physiology of bestrophins: multifunctional membrane proteins linked to Best Disease and other retinopathies. *Physiol. Rev.* In press.

Hazama, A., and Y. Okada. 1988. $Ca^{2+}$ sensitivity of volume-regulatory $K^+$ and $Cl^-$ channels in cultured human epithelial cells. *J. Physiol.* 402:687–702.

Hoffmann, E.K., and L.O. Simonsen. 1989. Membrane mechanisms in volume and pH regulation in vertebrate cells. *Physiol. Rev.* 69:315–382.

Jackson, A.L., J. Burchard, J. Schelter, B.N. Chau, M. Cleary, L. Lim, and P.S. Linsley. 2006. Widespread siRNA "off-target" transcript silencing mediated by seed region sequence complementarity. *RNA.* 12:1179–1187.

Jackson, P.S., and K. Strange. 1996. Single channel properties of a volume sensitive anion channel: lessons from noise analysis. *Kidney Int.* 49:1695–1699.

Jentsch, T.J., V. Stein, F. Weinreich, and A.A. Zdebik. 2002. Molecular structure and physiological function of chloride channels. *Physiol. Rev.* 82:503–568.

Kennedy, B.G. 1994. Volume regulation in cultured cells derived from human retinal pigment epithelium. *Am. J. Physiol.* 266:C676–C683.

Kim, M.J., G. Cheng, and D.K. Agrawal. 2004. $Cl^-$ channels are expressed in human normal monocytes: a functional role in migration, adhesion and volume change. *Clin. Exp. Immunol.* 138:453–459.

Kramer, F., K. White, D. Pauleikhoff, A. Gehrig, L. Passmore, A. Rivera, G. Rudolph, U. Kellner, M. Andrassi, B. Lorenz, et al. 2000. Mutations in the VMD2 gene are associated with juvenile-onset vitelliform macular dystrophy (Best disease) and adult vitelliform macular dystrophy but not age-related macular degeneration. *Eur. J. Hum. Genet.* 8:286–292.

Kulkarni, M.M., M. Booker, S.J. Silver, A. Friedman, P. Hong, N. Perrimon, and B. Mathey-Prevot. 2006. Evidence of off-target

effects associated with long dsRNAs in *Drosophila melanogaster* cell-based assays. *Nat. Methods.* 3:833–838.

la Cour, M., and T. Zeuthen. 1993. Osmotic properties of the frog retinal pigment epithelium. *Exp. Eye Res.* 56:521–530.

Lang, F., G.L. Busch, M. Ritter, H. Volkl, S. Waldegger, E. Gulbins, and D. Haussinger. 1998. Functional significance of cell volume regulatory mechanisms. *Physiol. Rev.* 78:247–306.

Marmorstein, A.D., L.Y. Marmorstein, M. Rayborn, X. Wang, J.G. Hollyfield, and K. Petrukhin. 2000. Bestrophin, the product of the Best vitelliform macular dystrophy gene (VMD2), localizes to the basolateral membrane of the retinal pigment epithelium. *Proc. Natl. Acad. Sci. USA.* 97:12758–12763.

Marmorstein, L.Y., J. Wu, P. McLaughlin, J. Yocom, M.O. Karl, R. Neussert, S. Wimmers, J.B. Stanton, R.G. Gregg, O. Strauss, et al. 2006. The light peak of the electroretinogram is dependent on voltage-gated calcium channels and antagonized by bestrophin (Best-1). *J. Gen. Physiol.* 127:577–589.

Marquardt, A., H. Stohr, L.A. Passmore, F. Kramer, A. Rivera, and B.H. Weber. 1998. Mutations in a novel gene, VMD2, encoding a protein of unknown properties cause juvenile-onset vitelliform macular dystrophy (Best's disease). *Hum. Mol. Genet.* 7:1517–1525.

McCarty, N.A., and R.G. O'Neil. 1992. Calcium signaling in cell volume regulation. *Physiol. Rev.* 72:1037–1061.

Moffat, J., J.H. Reiling, and D.M. Sabatini. 2007. Off-target effects associated with long dsRNAs in *Drosophila* RNAi screens. *Trends Pharmacol. Sci.* 28:149–151.

Moreland, J.G., A.P. Davis, G. Bailey, W.M. Nauseef, and F. Lamb. 2006. Anion channels, including ClC-3, are required for normal neutrophil oxidative function, phagocytosis, and transendothelial migration. *J. Biol. Chem.* 281:12277–12288.

Nilius, B., J. Eggermont, T. Voets, G. Buyse, V. Manolopoulos, and G. Droogmans. 1997. Properties of volume-regulated anion channels in mammalian cells. *Prog. Biophys. Mol. Biol.* 68:69–119.

Park, J.S., Y.J. Choi, V.J. Siegrist, Y.S. Ko, and W.K. Cho. 2007. Permissive role of calcium on regulatory volume decrease in freshly isolated mouse cholangiocytes. *Pflugers. Arch.* 455:261–271.

Petrukhin, K., M.J. Koisti, B. Bakall, W. Li, G. Xie, T. Marknell, O. Sandgren, K. Forsman, G. Holmgren, S. Andreasson, et al. 1998. Identification of the gene responsible for Best macular dystrophy. *Nat. Genet.* 19:241–247.

Qu, Z., R.W. Wei, W. Mann, and H.C. Hartzell. 2003. Two bestrophins cloned from *Xenopus laevis* oocytes express Ca-activated Cl currents. *J. Biol. Chem.* 278:49563–49572.

Qu, Z., Y. Cui, and C. Hartzell. 2006a. A short motif in the C-terminus of mouse bestrophin 4 inhibits its activation as a Cl channel. *FEBS Lett.* 580:2141–2146.

Qu, Z., L.T. Chien, Y. Cui, and H.C. Hartzell. 2006b. The anion-selective pore of the bestrophins, a family of chloride channels associated with retinal degeneration. *J. Neurosci.* 26:5411–5419.

Rosenthal, R., B. Bakall, T. Kinnick, N. Peachey, S. Wimmers, C. Wadelius, A. Marmorstein, and O. Strauss. 2005. Expression of bestrophin-1, the product of the VMD2 gene, modulates voltage-dependent $Ca^{2+}$ channels in retinal pigment epithelial cells. *FASEB J.* 20:178–180.

Ross, P.E., S.S. Garber, and M.D. Cahalan. 1994. Membrane chloride conductance and capacitance in Jurkat T-lymphocytes during cell swelling. *Biophys. J.* 66:169–178.

Rual, J.F., N. Klitgord, and G. Achaz. 2007. Novel insights into RNAi off-target effects using *C. elegans* paralogs. *BMC Genomics.* 8:106.

Sun, H., T. Tsunenari, K.-W. Yau, and J. Nathans. 2002. The vitelliform macular dystrophy protein defines a new family of chloride channels. *Proc. Natl. Acad. Sci. USA.* 99:4008–4013.

Svoboda, P. 2007. Off-targeting and other non-specific effects of RNAi experiments in mammalian cells. *Curr. Opin. Mol. Ther.* 9:248–257.

Szucs, G., S. Heinke, G. Droogmans, and B. Nilius. 1996. Activation of the volume-sensitive chloride current in vascular endothelial cells requires a permissive intracellular $Ca^{2+}$ concentration. *Pflugers Arch.* 431:467–469.

Tsien, R.Y., and T. Pozzan. 1989. Measurements of cytosolic free $Ca^{2+}$ with Quin-2. *Methods Enyzmol.* 172:230–262.

Tsunenari, T., H. Sun, J. Williams, H. Cahill, P. Smallwood, K.-W. Yau, and J. Nathans. 2003. Structure-function analysis of the bestrophin family of anion channels. *J. Biol. Chem.* 278:41114–41125.

Yardley, J., B.P. Leroy, N. Hart-Holden, B.A. Lafaut, B. Loeys, L.M. Messiaen, R. Perveen, M.A. Reddy, S.S. Bhattacharya, E. Traboulsi, et al. 2004. Mutations of VMD2 splicing regulators cause nanophthalmos and autosomal dominant vitreoretinochoroidopathy (ADVIRC). *Invest. Ophthalmol. Vis. Sci.* 45:3683–3689.

Yu, K., Y. Cui, and H.C. Hartzell. 2006. The bestrophin mutation A243V, linked to adult-onset vitelliform macular dystrophy, impairs its chloride channel function. *Invest. Ophthalmol. Vis. Sci.* 47:4956–4961.

Yu, K., Z. Qu, Y. Cui, and H.C. Hartzell. 2007. Chloride channel activity of bestrophin mutants associated with mild or late-onset macular degeneration. *Invest. Ophthalmol. Vis. Sci.* 48:4694–4705.